Magneto-optical transverse Kerr effect in multilayers

Carlos Dehesa-Martínez
ETS de Ingenieros de Telecomunicación, Universidad de Valladolid, Campus Miguel Delibes, 47011 Valladolid, Spain

L. Blanco-Gutierrez, M. Vélez, J. Díaz, L. M. Alvarez-Prado, and J. M. Alameda
Laboratorio de Magnetoóptica y Láminas Delgadas, Departamento de Física, Universidad de Oviedo, c/ Calvo Sotelo, s/n, 33007 Oviedo, Spain

(Received 15 December 2000; revised manuscript received 1 February 2001; published 20 June 2001)

We present detailed theoretical and experimental analysis of the magneto-optic transverse Kerr effect in magnetic multilayers. The theoretical model is based upon a phenomenological permittivity tensor. From the general result, suitable only for numerical calculations, we derive several approximate analytical expressions in order to make a qualitative discussion. The theoretical predictions are compared with experimental results in Y/Co bilayers, and the good agreement found allows for an accurate determination of the magneto-optical constants of the material. Then, the theoretical model is applied to make a detailed study of interface magnetism in $Y_{1-x}Co_x$ alloys, and to perform numerical simulations in Co/Cu and Fe/Cu multilayers. The results in multilayers highlight the complex behavior of the magneto-optic transverse Kerr effect, in which the contributions of the individual layers are never strictly additive. This nonlinearity is found to be strongly dependent on the $3d$ magnetic metal present and could be used to probe the alignment of the layers even in a configuration of vanishing magnetic moment.

DOI: 10.1103/PhysRevB.64.024417 PACS number(s): 75.70.Ak, 75.70.Cn

I. INTRODUCTION

Since the initial findings of Faraday and Kerr, the study of the magneto-optic effects has played an important role in the development both of electromagnetic theory and atomic physics. When applied to magnetically ordered media, magneto-optic spectrometry, from the near IR to the synchrotron radiation, is a powerful tool for the study of the electronic structure of these materials.[1–4] Besides that, magneto-optic effects are widely used as the basis of optical magnetometers, that provide a good sensitivity to measure both ultrathin films[5,6] or small areas of patterned structures,[7–10] and are easily implemented to perform *in situ* measurements in a variety of environments such as ultrahigh vacuum chambers.

Figure 1 shows the configurations for the most usual reflection magneto-optic effects (longitudinal, polar, and transverse Kerr effects).[11] The general condition for every reflection magneto-optic effect is that the incident electric field must have a component perpendicular to the sample magnetization. The longitudinal and polar effects produce a rotation of the polarization plane together with an ellipticity of the reflected light. (As a matter of fact, these effects are usually described as birefringence and circular magnetic dichroism, respectively). The last one is the magneto-optic transverse Kerr effect (MOTKE) and it is characterized by a small modulation of the reflectance caused by the component of the magnetization perpendicular to the optic plane when the incident light is *p* polarized. All of these effects have been successfully applied to the study of magnetic properties of bulk systems, such as magneto-optical constants or hysteresis loops.[12] Even, by the combination of several of the Kerr effects, multiple components of the magnetization can be measured on the same sample.[13] One of the main features of magneto-optical effects is that they provide information only of a surface layer of the order of the light penetration depth in the material. For this reason, some of their best fields of application in the last decade are in the study of magnetic multilayers[14–19] and in surface magnetism.[20]

In general, the magneto-optical response of a single magnetic layer is strongly dependent on the material electronic structure, light wavelength (λ), and on geometrical parameters such as the incidence angle or the layer thickness. The resulting behavior becomes increasingly complex for multilayer structures and, in many cases, the global sample response cannot be simply derived from that of the individual layers. However, this kind of structures, composed of more than a single semi-infinite layer, are precisely the ones where magneto-optical measurements reveal their power as an analytical tool to detect, for example, the presence of magnetic subsurface layers or to study the character of magnetic coupling (ferro- or antiferromagnetic) in magnetic multilayers.[23–27] Therefore, in order to obtain a reliable

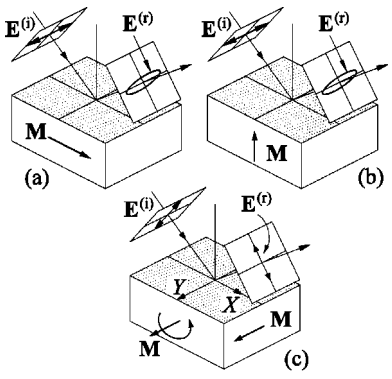

FIG. 1. Schematic of the three Kerr effect configurations. (a) Longitudinal. (b) Polar. (c) Transverse. The definition for a positive magnetization is also shown.

qualitative and quantitative information from the magneto-optical response of a multilayer structure a detailed theoretical model is necessary. A general formulation of the propagation of electromagnetic plane waves of arbitrary polarization in multilayered media requires the use of (4×4) dynamic matrices.[28] Computer simulations have been performed that include both first and second-order magneto-optic effects.[29] In general, most of the emphasis in the theoretical developments of magneto-optical effects in multilayers has been set in the study of the longitudinal and polar Kerr effects. In this case, it has been shown[30] that the contributions from the individual layers can be simply added to obtain the multilayer response, at least in the ultrathin-film limit. However, it has been pointed that care must be taken with the handling of spurious high-order terms in the (4×4)-matrix method.[31] These theoretical analysis have enabled a large body of experimental work, in which polar and longitudinal Kerr effects are used to determine the magnetic properties of thin films and multilayers such as interlayer coupling, magnetic phases, etc.[14,15,17,18,20–27] On the other hand, much less attention has been devoted to the study of the MOTKE in multilayers, even though it presents several advantages both from the theoretical and experimental point of view. First, the description of the light propagation in a magnetic medium in the transverse configuration is simpler than in the other configurations since only one linearly polarized plane wave is involved in any propagation direction. Then, for those cases of samples having the magnetization parallel to the reflection surface, the experimental setup needed for the detection of the MOTKE is simpler than that for measuring the longitudinal Kerr effect. These features of MOTKE have made it a widely used technique in other fields such as the study of magnetic nanostructures.[8–10]

In this work, we present a detailed theoretical analysis of the MOTKE in magnetic multilayers based upon a phenomenological permittivity tensor, that allows to obtain the MOTKE response of arbitrary multilayers in terms of the properties of the individual layers. The obtained results are, in general, only suitable for numerical analysis. However, in some simple cases approximate expressions can be derived and a qualitative discussion is possible. The predictions from the theoretical model will be compared with the experimental MOTKE behavior in particular multilayer structures of the Y/Co system. The observed behavior presents fundamental differences with the other two linear Kerr effects, the multilayer response is often highly nonlinear, and there is not, in general, an additivity rule between the contributions of the individual layers even in the thin-film limit. It will be shown how the comparison between theory and experiment results in an accurate determination of the magneto-optical constants of the material, and how the differences that may appear can be discussed in terms of interface magnetism. Finally, the behavior of MOTKE in multilayers with small modulations and the issue of additivity between the contributions from the individual layers response will be addressed by numerical simulations in the Co/Cu and Fe/Cu systems.

The paper is organized as follows. In Sec. II the experimental setup for sample growth and MOTKE characterization is described. In Sec. III we will deal with the theoretical analysis of the transverse Kerr effect in multilayer magnetic structures. Section IV corresponds to the analysis of some simple structures, illustrated with experimental examples in the Y/Co system. Then, in Sec. V, our model will be applied to the experimental study of surface magnetism in $Y_{1-x}Co_x$ alloys. Section VI is devoted to the theoretical analysis of multilayers in the Co/Cu and Fe/Cu systems. The conclusions are presented in Sec. VII. Finally, the detailed approximate analysis of the behavior of a magnetic film on a metal substrate will be carried out in the Appendix.

II. EXPERIMENT

Multilayered Y/Co/Nb and amorphous Y_xCo_{1-x} samples were grown by means of co-magnetron sputtering with independent pure Y, Co, and Nb targets in a vacuum chamber with a base pressure of 10^{-9} mbar and an Ar working pressure of 10^{-3} mbar. The Ar used was 99.99% pure. The substrates were either corning glass or Si(100) at room temperature. Thickness was monitored *in situ* by a quartz microbalance and calibrated by a surface profilometer, while composition was checked by electron probe x-ray microanalysis. Two different experimental setups were used for the MOTKE measurements, with a similar geometry as reported earlier.[32] One of them is installed in the deposition chamber in order to perform measurements in vacuum while the other works in air (later they will be referred to as *in situ* and *ex situ* setups, respectively). Briefly, the incident light beam was linearly polarized parallel to the plane of incidence, and the reflected light was detected with a *p-i-n* photodiode with a peak sensitivity at 900 nm and with a spectral response lying in the 500–1200 nm range. Measurements were carried out with monochromatic light from a laser diode with $\lambda=670$ nm and 0.5 mW of power, except in some special cases where a lamp source (3000 K, radiating in the 500–2000 nm range) was used. A magnetic field was applied perpendicular to the plane of incidence in order to perform the MOTKE hysteresis loops. The photodiode voltage signal at zero field was taken as a measure of the sample reflectivity R. Then, this continuous signal was electronically compensated, and the total change in reflectivity ΔR from positive to negative saturation was recorded as a function of magnetic field, averaging over several field loops in order to improve the signal-to-noise ratio. The main difference between the two experimental systems used in this work is that in the *in situ* setup the angle of incidence is fixed at $\theta=30°$, while in the *ex situ* setup θ can be varied in a broad angular range. Auxiliary bulk-magnetization measurements were carried out by means of alternating-gradient magnetometry (AGM).[33]

III. TRANSVERSE KERR EFFECT IN MULTILAYER STRUCTURES

A. Some definitions

The magneto-optic transverse Kerr effect can be phenomenologically described by a parameter δ_K, defined as

$$\delta_K=\frac{R_+-R_-}{R}, \tag{1}$$

where $R_+ - R_-$ is the change in reflectance caused by an inversion of the sample transverse magnetization, from **M** to $-\mathbf{M}$, and R is the reflectance for an ideal demagnetized sample, experimentally represented by the average value of R_+ and R_-. Typical values of δ_K for 3*d* magnetism range from 10^{-3} to 10^{-2}. We define the magnetization as positive, with the corresponding R_+, when it can be attributed to Amperian currents rotating in the same sense as the light beam does upon reflection, as it can be seen in Fig. 1(c), where the coordinate system used through this paper is also shown.

The time dependence of the light field will be described, according to the notation used in Ref. 30, by the factor $\exp(-i\omega t)$. Other authors, as in Refs. 34 and 35, prefer to use $\exp(i\omega t)$. To match their results and ours, one has just to substitute i for $-i$ in all expressions, i.e., to take the complex conjugate in all of them. For isotropic media magnetized along the OY axis, the permittivity tensor is given by:[30]

$$\bar{\varepsilon} = \varepsilon_0 N^2 \begin{bmatrix} 1 & 0 & -iQ \\ 0 & 1 & 0 \\ iQ & 0 & 1 \end{bmatrix}, \tag{2}$$

where $N = n + i\kappa$ and Q are the complex refractive index and the magneto-optic constant, respectively. Generally, $|Q| \ll 1$. For a nonmagnetic layer $Q = 0$, and for a transparent one $\kappa = 0$. At optical frequencies, the magnetic permeability, μ, is usually assumed to be equal to that of the vacuum, μ_0.[36]

B. Preliminary analysis of the MOTKE in thick layers

A theoretical expression for δ_K in semi-infinite homogeneous magnetic samples has been deduced by several authors.[12,34,35] For monochromatic light incident from a transparent medium 1 into a magnetic medium 2, δ_K is given by[11]

$$\delta_K = 4N_1^2 \sin 2\theta_1 \, \mathrm{Re}\left(\frac{iN_2^2 Q_2}{(N_2^4 - N_1^4)\cos^2\theta_1 - N_1^2 N_2^2 + N_1^4} \right), \tag{3}$$

where θ_1 is the angle of incidence, and only terms linear in Q have been considered. More details on the derivation of this equation are given in Sec. IV A.

Experimentally, a maximum of δ_K vs θ_1 is observed for $\theta_1 > 45°$, in agreement with Eq. (3), since for magnetic conductors $|N^2| \gg 1$. Equation (3) implies a direct relation between δ_K and the material magnetization M since, for a given material and wavelength, perturbative analysis[12] has shown Q to be linear in M. However, this first-order linearity is to be cautiously extrapolated to real materials since the experimental relations between Q and M are usually found to contain also higher orders in M.[37] Also, the dependence of δ_K on λ and material is not straightforward mainly due to the nontrivial dependence of QN^2 on λ that contains information on magneto-optic transitions related to the electronic band structure of the medium. For instance, even sign changes in δ_K were early observed in the IR-VIS part of the spectrum on 3*d* metals.[34]

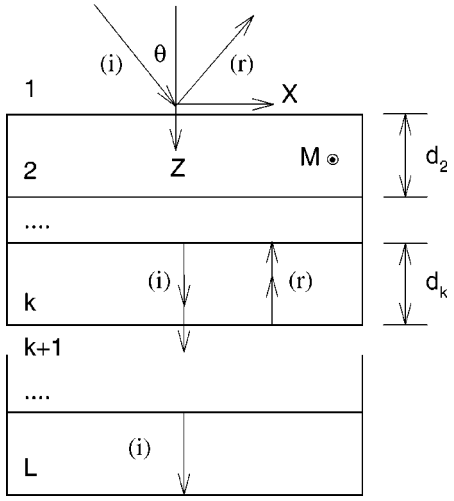

FIG. 2. A multilayer structure in the transverse Kerr configuration with a positive magnetization. The OY axis points outward the figure. The plane XZ is the optic or incidence plane.

The complex magneto-optic parameter Q is experimentally obtained from measurements of δ_K at two values of the angle of incidence and Eq. (3), assuming a previous knowledge of the refractive index N of the medium.[34,35,37]

C. Plane-wave propagation in an isotropic magnetic medium magnetized in the transverse Kerr configuration

In our analysis we study the propagation of plane waves in layered structures according to Maxwell equations, where each medium is represented by a permittivity tensor. At the boundaries between homogeneous layers we impose the usual conditions of continuity of tangential components of the **E** and **H** fields. It has to be noted that any kind of MOTKE observed in multilayers that cannot be described within this framework must be related with interface effects, such as the presence of quantum-well states[38] or interdiffusion that result in less-well-defined boundaries between the different layers. A schematic representation of the multilayer structure, constituted by homogeneous media, and the coordinate system used in this paper is shown in Fig. 2.

First, let us analyze the propagation of plane monochromatic waves through any of these layers. Since the time dependence of fields is taken as $\exp(-i\omega t)$, Maxwell equations can be written in the form

$$\nabla \times \mathbf{E} = i\omega\mu_0 \mathbf{H} \quad \text{and} \quad \nabla \times \mathbf{H} = -i\omega \mathbf{D}, \tag{4}$$

where $\mathbf{D} = \bar{\varepsilon}\mathbf{E}$ and $\bar{\varepsilon}$ is given by Eq. (2). From them, one immediately deduces that $\nabla \cdot \mathbf{H} = 0$ and $\nabla \cdot \mathbf{D} = 0$.

We will write the wave field spatial dependence as $\exp[i(\omega/c)\mathbf{n}\cdot\mathbf{r}]$, where, for metal media, the propagation vector **n** is going to be complex. For those plane waves, we can substitute $i(\omega/c)\mathbf{n}$ for the symbol ∇ in Maxwell equations, resulting

$$\mathbf{H} = \frac{1}{\mu_0 c}\mathbf{n} \times \mathbf{E} \tag{5}$$

and

$$\mathbf{D} = -\frac{1}{c}\mathbf{n}\times\mathbf{H}. \tag{6}$$

The last equation means that $\mathbf{n}\cdot\mathbf{D}=0$. By eliminating $\mathbf{H}$ between Eqs. (5) and (6) we get a homogeneous equation for $\mathbf{E}$

$$\overline{\varepsilon}\mathbf{E} = -\varepsilon_0\mathbf{n}\times(\mathbf{n}\times\mathbf{E}). \tag{7}$$

Since we are taking XZ as the optic plane, the continuity condition for the tangential components of the $\mathbf{E}$ and $\mathbf{H}$ fields at the boundaries, parallel to the plane $z=0$, implies that the components n_x and n_y of the propagation vector have the same value in the whole structure, equal to their values in the incidence medium, so that

$$n_x = N_1 \sin\theta_1 \quad \text{and} \quad n_y = 0, \tag{8}$$

where N_1 and θ_1 represent the refractive index for the first medium and the light incidence angle, respectively. Then

$$\mathbf{n} = \hat{\mathbf{x}}n_x + \hat{\mathbf{z}}n_z. \tag{9}$$

Hence, the compatibility condition for Eq. (7) is

$$\begin{vmatrix} N^2-n_z^2 & 0 & n_xn_z - iQN^2 \\ 0 & N^2-n^2 & 0 \\ n_zn_x + iQN^2 & 0 & N^2-n_x^2 \end{vmatrix} = 0, \tag{10}$$

which determines the possible values for $\mathbf{n}$ squared as

$$n^2 = \begin{cases} N^2 \\ N^2(1-Q^2) \end{cases}. \tag{11}$$

Going back to Eq. (7), we see that the first value of n^2 corresponds to a *s*-polarized wave, i.e., one with the electric field linearly polarized along the axis normal to the optic plane (OY axis). The associated magnetic field, given by Eq. (5), is seen to be independent of the magneto-optic constant. Since both the fields and the propagation vector are Q independent, we see that there is no transverse Kerr effect for this polarization.

For $n^2 = N^2(1-Q^2)$, Eq. (7) determines that the wave electric field is placed on the optic plane (polarization *p*). According to Eq. (5), the magnetic field appears necessarily perpendicular to the optic plane. Once the value of n_x is fixed by the incident wave, the component n_z of the propagation vector can take two opposite values that correspond to waves traveling along both directions of the OZ axis. Therefore, the *p*-polarized waves propagate along the different layers, all of which are supposed magnetized in the transverse configuration without any change in polarization and are always linear.

Therefore, if the magnetic field amplitude is

$$\mathbf{H} = \hat{\mathbf{y}}H_y \exp[i(\omega/c)\mathbf{n}\cdot\mathbf{r}] \tag{12}$$

the corresponding electric field amplitude in the same medium can be obtained from Eqs. (6) and (2), and is given by

$$\mathbf{E}(\mathbf{r}) = \frac{1}{\varepsilon_0 cN^2}\left[\hat{\mathbf{x}}\frac{n_z - iQn_x}{1-Q^2} - \hat{\mathbf{z}}\frac{n_x + iQn_z}{1-Q^2}\right]H_y \times \exp[i(\omega/c)\mathbf{n}\cdot\mathbf{r}], \tag{13}$$

where $1-Q^2 \cong 1$ is generally accomplished for $3d$ magnetic elements. This approximation will also hold even in the heavy-element containing systems that produce some of the largest polar Kerr rotations, such as the Heusler alloys, where Q is smaller than 10^{-1} at least for wavelengths in the visible range.[39]

D. Analysis of propagation in a multilayered structure

As previously said, the reflectance for *s* polarized light does not change when the magnetization direction is reversed in the transverse Kerr configuration. Then, for any direction of propagation one has to consider only one linearly polarized wave with its electric field in the plane of incidence (*p* polarized light). The wave in any layer can be described as a superposition of incident and reflected waves, each *p* polarized. Let us consider a multilayered structure with L layers, as shown in Fig. 2, where d_k is the thickness of the kth layer. The extreme media, 1 and L, represent the incidence medium, usually air, and a very thick absorbing medium, respectively. Except for layer L, where only an incident wave propagates, the wave field in every layer is the sum of two plane waves, the incident *i* and the reflected *r*. To simplify notation, we will agree to place the origin for coordinate z in each layer at its upper surface, except for medium 1, where $z=0$ is the boundary plane with the second medium The magnetic field for the wave in the kth layer is the sum of the incident and reflected fields given by

$$\mathbf{H}_k^{(i,r)}(\mathbf{r}) = \hat{\mathbf{y}}H_k^{(i,r)} \exp[i(\omega/c)\mathbf{n}_k^{(i,r)}\cdot\mathbf{r}]. \tag{14}$$

For a positive magnetization, the electric fields of the waves, from Eq. (13), are given by the expression

$$\mathbf{E}_k^{(i,r)}(\mathbf{r}) = \frac{H_k^{(i,r)}}{\varepsilon_0 cN_k^2}[\hat{\mathbf{x}}a_k^{(i,r)} + \hat{\mathbf{z}}b_k^{(i,r)}]\exp[i(\omega/c)\mathbf{n}_k^{(i,r)}\cdot\mathbf{r}], \tag{15}$$

where

$$a_k^{(i,r)} = n_{k,z}^{(i,r)} - iQ_kn_x \tag{16}$$

and

$$b_k^{(i,r)} = -(n_x + iQ_kn_{k,z}^{(i,r)}). \tag{17}$$

In the last two equations it has been taken into account that n_x is constant along the whole structure and is given by

$$n_x = N_1 \sin\theta_1. \tag{18}$$

Moreover, from Eq. (11), in which $|Q|^2 \ll 1$, we can derive the values for the normal component of $\mathbf{n}_k$ corresponding to the incident and reflected waves as

$$n_{k,z}^{(i,r)} = \pm\sqrt{N_k^2 - n_x^2}. \tag{19}$$

As seen in Eq. (15), each component of the electric field is proportional to the corresponding magnetic field amplitude. Therefore, both boundary conditions can be stated in terms of the incident and reflected magnetic field amplitudes only. At each layer, we build a column matrix with the magnetic field amplitudes at its upper surface, $z=0$:

$$\mathbf{H}_k=\begin{bmatrix} H_k^{(i)} \\ H_k^{(r)} \end{bmatrix}, \quad k=1,2,\ldots,L. \tag{20}$$

At the last medium $H_L^{(r)}=0$, since it is assumed that there is no reflected wave. The conditions at the boundary between kth and $k+1$th layers can be set in matrix form as

$$\mathbf{A}(k\rightarrow k+1)\mathbf{H}_k=\mathbf{B}(k\rightarrow k+1)\mathbf{H}_{k+1}, \quad k=1,2,\ldots,L-1, \tag{21}$$

where $\mathbf{A}(k\rightarrow k+1)$ and $\mathbf{B}(k\rightarrow k+1)$ are the matrices

$$\mathbf{A}(k\rightarrow k+1)=\begin{bmatrix} \exp\left[i\left(\frac{\omega}{c}\right)n_{k,z}^{(i)}d_k\right] & \exp\left[-i\left(\frac{\omega}{c}\right)n_{k,z}^{(i)}d_k\right] \\ \frac{a_k^{(i)}}{N_k^2}\exp\left[i\left(\frac{\omega}{c}\right)n_{k,z}^{(i)}d_k\right] & \frac{a_k^{(r)}}{N_k^2}\exp\left[-i\left(\frac{\omega}{c}\right)n_{k,z}^{(i)}d_k\right] \end{bmatrix}, \quad k=2,\ldots,L-1, \tag{22}$$

$$\mathbf{A}(1\rightarrow 2)=\begin{bmatrix} 1 & 1 \\ \cos\theta_1/N_1 & -\cos\theta_1/N_1 \end{bmatrix}, \tag{23}$$

and

$$\mathbf{B}(k\rightarrow k+1)=\begin{bmatrix} 1 & 1 \\ a_{k+1}^{(i)}/N_{k+1}^2 & a_{k+1}^{(r)}/N_{k+1}^2 \end{bmatrix}, \quad k=1,\ldots,L-1. \tag{24}$$

Since matrices $\mathbf{A}$ are invertible, we can get $\mathbf{H}_k$ from Eqs. (21), as

$$\mathbf{H}_k=\mathbf{A}(k\rightarrow k+1)^{-1}\mathbf{B}(k\rightarrow k+1)\mathbf{H}_{k+1} \tag{25}$$

and eliminate all the intermediate matrices $\mathbf{H}_k$ ($k=2,\ldots,L$-1) that appear in Eqs. (21), to obtain

$$\mathbf{H}_1=\mathbf{A}(1\rightarrow 2)^{-1}\mathbf{B}(1\rightarrow 2)\mathbf{A}(2\rightarrow 3)^{-1} \times\mathbf{B}(2\rightarrow 3)\cdots\mathbf{A}(L-1\rightarrow L)^{-1}\mathbf{B}(L-1\rightarrow L)\mathbf{H}_L, \tag{26}$$

representing a two-equation system from which we can eliminate the last medium amplitude, $H_L^{(i)}$, and obtain the amplitude reflection coefficient, $r_+=H_1^{(r)}/H_1^{(i)}$. The reflectance for positive magnetization is, finally,

$$R_+=\left|\frac{H_1^{(r)}}{H_1^{(i)}}\right|^2. \tag{27}$$

To obtain R_- suffice it to repeat Eq. (26) replacing every Q_k with $-Q_k$ and to follow the indicated steps up to Eq. (27). The parameter δ_K is then readily obtained from its definition given by Eq. (1), where R can be deduced as R_+ by taking every $Q_k=0$.

In the following sections this model will be applied for the simulation of the magneto-optical behavior of a variety of multilayered structures. We have taken the usual approximation[20] of considering the values of the optical refractive indexes and magneto-optical constants indicated in tables for bulk materials,[34,40] which are given in Table I. There are some cases, that will be explicitly noted, where N_k or Q_k are used as fit parameters in order to obtain more accurate values. In the ultrathin-film limit, some changes in these constants could be expected due to electronic redistribution and interface effects. These could be implemented in our model, whenever it would be found necessary to explain the detailed magnetic response of a particular multilayer system, by introducing a thickness dependence of the constants for films in the 1–2 nm range, in a similar way as done by Atkinson and Dodd in studies of polar Kerr effect in Co/Cu multilayers.[41]

IV. RESULTS FOR SOME SIMPLE STRUCTURES

The former analysis is well suited to obtain numerical results on a computer for specific structures and materials. Nevertheless, detailed expressions for δ_K are cumbersome and therefore do not permit to draw from them a qualitative physical insight. An important exception is the case of a

TABLE I. Optic and magneto-optic data for the materials cited in this paper at $\lambda=670$ nm taken from Refs. 34 and 40.

	n	κ	Q
Fe	2.93	3.10	$0.007\,49+0.0225i$
Co	2.25	4.27	$0.021-0.007i$
Ni	1.96	4.02	$0.009\,30-0.006\,22i$
Y	2.11	2.40	0
Nb	2.67	2.92	0
Cu	0.216	3.386	0
Si	3.821	0.015	0

single thick magnetic layer for which relative simple analytical expression exists. By taking a simple approximation, this expression for δ_K can be adapted to metal structures with a single thin magnetic layer on a metallic substrate and a physical discussion of the results is then possible. The resulting behavior will be illustrated with experimental results in the Y/Co system.

A. Thick magnetic layer

For incidence from a vacuum, or from air, onto a semi-infinite magnetic layer, with complex refractive index N_2 and magneto-optic constant Q_2, the light magnetic field in the first medium can be written, according to Eq. (26) in the form

$$\mathbf{H}_1 = \mathbf{A}(1\rightarrow 2)^{-1}\mathbf{B}(1\rightarrow 2)\mathbf{H}_2, \tag{28}$$

where matrices $\mathbf{A}(1\rightarrow 2)$ and $\mathbf{B}(1\rightarrow 2)$ are defined in Eqs. (23) and (24), respectively. The reflection coefficients can be written as

$$r_{\pm} = \frac{a \pm bQ_2}{c \pm dQ_2}, \tag{29}$$

where $a,c = N_2^2 \cos\theta_1 \mp (N_2^2 - \sin^2\theta_1)^{1/2}$ and $b = -d = i\sin\theta_1$. For an assumed zero magnetization, the reflection coefficient is obviously $r = a/c$. From its definition in Eq. (1), keeping only those terms linear in Q_2, the expression for δ_K is readily obtained,

$$\delta_K = 4\ \mathrm{Re}\left(\frac{bc-ad}{ac}Q_2\right) = 4\sin 2\theta_1\ \mathrm{Re}\frac{iQ_2N_2^2}{N_2^4\cos^2\theta_1 - N_2^2 + \sin^2\theta_1}. \tag{30}$$

Of course, this result is the same as given in Eq. (3) if $N_1 = 1$. In terms of the real and imaginary parts of the permittivity tensor elements, $\varepsilon_d \equiv N_2^2 = \varepsilon_d' + i\varepsilon_d''$ and $\varepsilon_{nd} \equiv iQ_2N_2^2 = \varepsilon_{nd}' + i\varepsilon_{nd}''$, this result can be written as

$$\delta_K = 4\sin 2\theta_1 \frac{G\varepsilon_{nd}' + K\varepsilon_{nd}''}{G^2+K^2}, \tag{31}$$

where

$$G = (\varepsilon_d'^2 - \varepsilon_d''^2 - 1)\cos^2\theta_1 - \varepsilon_d' + 1 \tag{32}$$

and

$$K = \varepsilon_d''(2\varepsilon_d'\cos^2\theta_1 - 1). \tag{33}$$

Equation (31) has been used to obtain the values of ε_{nd}' and ε_{nd}'' from the measured values of δ_K at two incident angles. More details on this method can be found, for instance, in Refs. 35 and 37.

By comparing expressions (3) and (30), for the case of light coming from a dielectric medium the value of δ_K appears enhanced by a factor approaching N^2 with respect to the incidence from air for a wide range of values of θ_1. However, if light comes from air through a thick dielectric slab, like a glass substrate, the angle of incidence on the magnetic medium will be reduced, according to Snell's law, which in most cases will signify a lowering of the value of the measured δ_K. If one wants to take advantage of the above-indicated increase of δ_K, it will prove suitable to prepare the sample on a prismatic glass substrate.[42] Finally, we would like to point out that the addition of an antireflexive coating produces, for the proper angle of incidence, a very large increment on δ_K which, obviously, is devoid of any magneto-optical significance.

B. Thin metal layer on a metallic substrate

As noted, there is no simple expression for δ_K in these cases. However, the simplifying assumption of taking the complex refractive indices of both media equal, i.e., $N_2 = N_3$, leads to a useful and interesting result. Of course, the calculated reflectance of the metal surface could differ largely from the measured one, but the quantity of concern here is δ_K, which is scarcely dependent on the difference between indices. This approach was introduced by Zak *et al.*,[43] in relation to the study of polar Kerr effect in multilayers.

Let Q_2 and Q_3 be the magneto-optic constants of the thin layer and substrate, respectively, and d the layer thickness. After a long but straightforward calculation, similar to the one outlined in the previous section, one obtains the same expression for δ_K as given by Eq. (30) in which Q_2 is replaced by an effective constant

$$Q_{\mathrm{eff}} = Q_2\left[1 - \left(1 - \frac{Q_3}{Q_2}\right)\exp\left(i\frac{2\omega n_{2,z}d}{c}\right)\right]. \tag{34}$$

In particular, for a protective metal coating over a magnetic substrate, $Q_2 = 0$,

$$Q_{\mathrm{eff}} = Q_3\exp\left(i\frac{2\omega n_{2,z}d}{c}\right). \tag{35}$$

In a similar way, for a thin-magnetic film on a metal substrate, where $Q_3 = 0$

$$Q_{\mathrm{eff}} = Q_2\left[1 - \exp\left(i\frac{2\omega n_{2,z}d}{c}\right)\right]. \tag{36}$$

Leaving aside a phase factor, the exponential factor in the last expressions uniformly decreases with the layer thickness d as $\exp(-4\pi\kappa d/\lambda)$. This fact can lead to the intuitive obvious idea that an increase in the thickness of a protective metal coating implies a decrease in the value δ_K, or that when a magnetic film is grown on a nonmagnetic substrate δ_K will increase smoothly up to the bulk value for a thick enough magnetic film. However, the mentioned phase factor, that depends on d also, may lead to a variety of anomalous effects, that can be easily illustrated in the Y/Co system.

Figure 3 shows the experimental δ_K values for a Y(d)/Co(48 nm)/Si(substrate) sample as a function of Y layer thickness (d_Y). The thickness of the Co layer has been chosen to be larger than the light-penetration depth so that

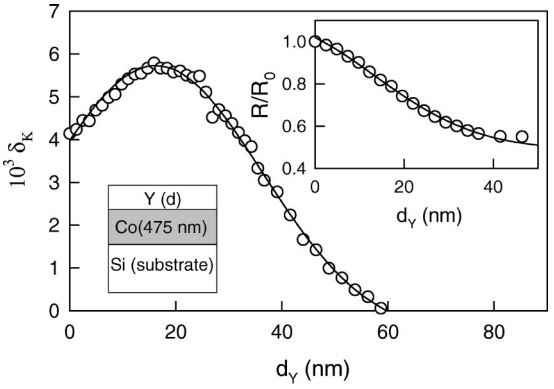

FIG. 3. δ_K vs Y-layer thickness for an Y(d)/Co(48 nm)/Si(substrate) sample, at an incidence angle $\theta=30°$. Solid line is a fit to the theoretical model of Sec. III, using as fit parameters N_Y and Q_{Co}. Inset shows the Y-layer thickness dependence of the reflectivity normalized by R_0, i.e., the value at $d_Y=0$. The solid line has been calculated using the optical constants of Y and Co obtained from the fit of δ_K vs d_Y. Also shown is a sketch of the sample structure.

this sample can be effectively considered as a Y(film)/Co(substrate) structure from the magneto-optical point of view. Measurements were taken at an incidence angle $\theta=30°$, with monochromatic light ($\lambda=670$ nm) using the *in situ* MOTKE setup described in Sec. II, so that all the experimental points correspond to the same sample. The observed behavior is clearly different from the intuitively expected attenuation due to the capping layer. For very small Y layer thickness, δ_K is enhanced for increasing d_Y, reaching a maximum at $d_Y=18$ nm. This qualitative behavior can be predicted from the Q_{eff} approach if the phase factor is properly taken into account. Details and further examples can be found in the Appendix. On the other hand, the full numerical model proposed in the previous section must be used to fit the δ_K vs d_Y curve, as indicated by the solid line in Fig. 3. In this calculation we have taken the refractive index of Co (N_{Co}) from Table I, while the refractive index of yttrium N_Y and the magneto-optical constant of Co (Q_{Co}) have been used as fit parameters. The resulting values are $N_Y=2.28+2.07i$ and $Q_{Co}=0.042-0.020i$. The fitted value of N_Y is comparable to the tabulated $N_Y=2.11+2.4i$. Even more, if the sample reflectivity vs d_Y dependence is calculated using the value of N_Y obtained from the fit, it is found to be in very good agreement with the experimental curve (see inset of Fig. 3). The main difference with the tabulated values is found for Q_{Co} ($Q_{Co}=0.021-0.007i$ was reported by Krinchik and Nurmukhamedov[34]). However, it is worth to note that here the magneto-optical constant is obtained from the fit of δ_K in a broad thickness range, which results in a more accurate determination than the standard method based on just two values of δ_K measured at two different angles for a bulk sample, mentioned in Sec. IV A.

The magneto-optical behavior of the complementary structure Co(film)/Y(substrate) is shown in Fig. 4. In this case, the samples are Co(d)/Y(100 nm)/glass(substrate) structures, however the yttrium underlayer thickness of 100 nm is thick enough to have the case of a thin magnetic layer

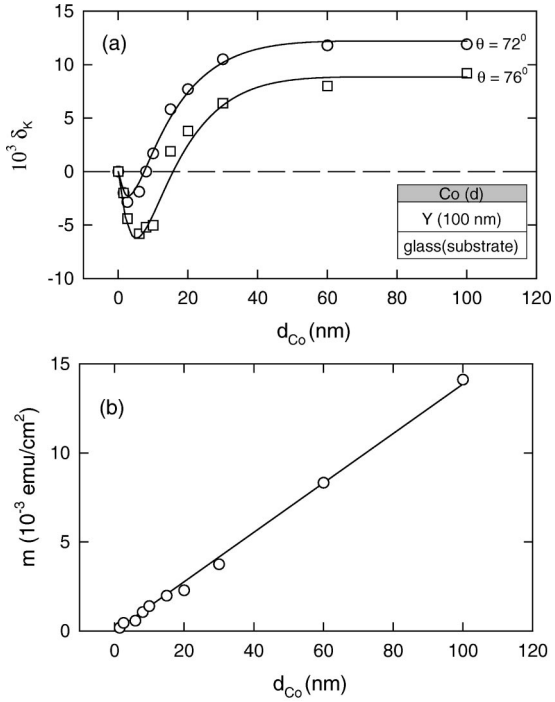

FIG. 4. (a) δ_K vs Co-layer thickness for Co(d)/Y(100 nm)/glass(substrate) samples measured at two incidence angles $\theta=72°$ (circles) and $\theta=76°$ (squares). Solid lines are fits to the theoretical model of Sec. III, using as fit parameter Q_{Co}. Also shown is a sketch of the samples structure. (b) Magnetic moment per surface unit vs Co thickness in these Co/Y samples measured by AGM. A linear fit is also shown.

grown on a conductive and optically absorbent medium. Measurements were made at two different incidence angles and with monochromatic light ($\lambda=670$ nm) at the *ex situ* setup. Each experimental point corresponds to a different sample so that a direct comparison between magneto-optical and bulk-magnetization measurements could be performed. Once again, the δ_K versus d_{Co} curve presents a peculiar behavior: δ_K is negative for small d_{Co}, crosses zero (at $d_{Co}\approx 15$ nm for $\theta=76°$) and finally it becomes positive and reaches the saturation bulk value for d_{Co} above 60 nm. This behavior does not mean that the Co samples are magnetically anomalous. The magnetic moment per surface unit, measured by AGM, clearly scales with cobalt thickness [see Fig. 4(b)]. Then, it is found that due to the phase factor in Eq. (36), vanishing δ_K values appear for obviously magnetic samples.

The nonlinear behavior of δ_K with Co thickness is a feature that makes difficult the use of MOTKE as an optical magnetometer in multilayered systems. On the other hand, this complex behavior is very sensitive to sample structure and allows for an accurate determination of the magneto-optical parameters of the material. The solid line in Fig. 4(a) corresponds to a fit of the experimental results to the numerical model of Sec. III. A good agreement is observed between theory and experiment in the whole Co thickness range considered. This suggests that our macroscopic approach is valid even at values of d_{Co} under 5 nm and that the Co layers are continuous at such thicknesses. In this case, we have used

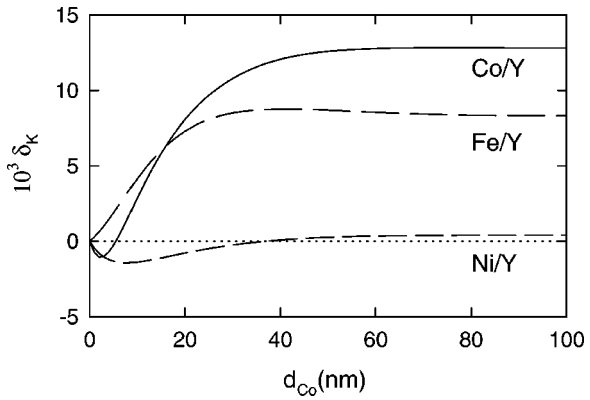

FIG. 5. Simulated δ_K vs magnetic film thickness for Co(d)/Y(substrate), Fe(d)/Y(substrate) and Ni(d)/Y(substrate) structures, with $\theta=70°$.

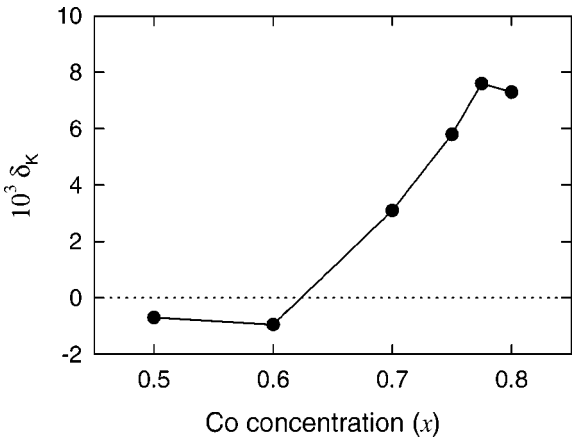

FIG. 6. δ_K vs Co concentration x for a thick $Y_{1-x}Co_x$ alloy measured at $\theta=68°$. Note the sign change in δ_K for $x=0.65$.

the same refractive indexes for the Y and Co layer as in the Y(film)/Co(substrate) structures of the previous example, while Q_{Co} has been used as a fit parameter. The resulting value is $Q_{Co}=0.042-0.014i$ which is indeed very similar to the previously obtained value of $Q_{Co}=0.042-0.020i$. Therefore, in the rest of the paper the value of $Q_{Co}=0.042-0.014i$ will be used in the simulations.

In general, the qualitative behavior observed in Figs. 3 and 4 for Co/Y structures is to be cautiously extrapolated to the cases of other materials. Figure 5, shows the simulated dependence of δ_K against thickness of the magnetic layer, for Co(film)/Y(substrate), Fe(film)/Y(substrate), and Ni(film)/Y(substrate) structures. The angle of incidence is $\theta_i=70°$ and the wavelength λ is 670 nm. The most influential factor in the values of δ_K is the 3d magnetic metal present. A sign change is observed for the Co and Ni layers while for the Fe structure there is an initial linear dependence for small thickness. The shape of each curve depends also on the incidence angle, so that the amplitude of the positive and negative δ_K values can be of a similar magnitude (see, e.g., Fig. 4). In any case, the sign reversal behavior is not very sensitive to small changes in the magneto-optical constants of the 3d material. This qualitative dependence can be derived using the approximate analytical expressions (35) and (36), even though the actual behavior must be obtained from exact equations of Sec. III D. The discussion about the conditions for sign change of δ_K on account of the 3d magnetic metal used, will be established in the Appendix, in the framework of Eq. (34).

The behavior of structures A/B, where A and B are both magnetic metals, is more predictable. In most cases, for a variation in the thickness of the upper layer, a monotonous variation of δ_K, between the bulk values for A and B, is to be found. Note, however, that a shallow relative maximum or minimum in δ_K for an intermediate thickness is also possible. Both experimental results for amorphous NdFeB/FeB bilayers and theoretical ones for amorphous FeSi/FeSi bilayers can be found in Ref. 44.

V. MOTKE AS A SURFACE PROBE IN AMORPHOUS $Y_{1-x}Co_x$ ALLOYS

The nonlinear behavior of MOTKE seems a little inconvenience, due to its complexity. But the fact that MOTKE is a surface probe, together with its nonlinear behavior, makes MOTKE a great experimental tool to analyze surface and interface magnetism. In the next example of $Y_{1-x}Co_x$ alloys we will show how this study can be very useful in the interpretation of experimental results commonly attributed to nonintentional interfaces, changes in interfacial magnetic coupling, etc., specially when combined with magnetometric measurements.

Starting from volume magnetometric measurements taken on amorphous $Y_{1-x}Co_x$ alloys at room temperature, it was found that these alloys are not magnetically ordered below $x=0.65$, and that above this cobalt concentration they present magnetic order.[45] However, an anomalous behavior of δ_K versus cobalt concentration was reported (as shown in Fig. 6). A nonvanishing and negative δ_K value appeared for alloys with $x<0.65$, in contradiction with the magnetometry measurements. This feature was explained in terms of selective Y oxidation that induces Y segregation to the surface, leaving a Co-enriched sublayer 3–4 nm thick, and thus ordered at room temperature. Using MOTKE it was verified that this Co sublayer is located at the film-air interface and not at the film-substrate interface. This process was also verified from magnetic properties, such as coercive force and anisotropy field.[45] However, the physical origin of the sign change in δ_K at $x<0.65$ was not clear. The results in the Co(film)/Y(substrate) structure of Fig. 4 offer a simple explanation, i.e., a very thin cobalt layer grown on a nonmagnetic conductor (i.e., $Y_{0.5}Co_{0.5}$), gives a negative δ_K. To experimentally establish this hypothesis on $Y_{0.5}Co_{0.5}$, an experiment has been carried out. Co(d)/$Y_{0.5}Co_{0.5}$(100 nm)/glass samples have been grown with a thick enough $Y_{0.5}Co_{0.5}$ layer so that they can be effectively considered as Co(film)/$Y_{0.5}Co_{0.5}$(substrate) structures. Their MOTKE has been measured at the same experimental conditions as in the $Y_{1-x}Co_x$ data of Ref. 45. The results correspond to the filled symbols in Fig. 7(a). δ_K is negative below $d_{Co}=5$ nm, and remains constant below 2 nm. The δ_K value at $d_{Co}=2$ nm ($\delta_K=-7.4\times10^{-4}$) is the same as that obtained in simple $Y_{0.5}Co_{0.5}$ samples. This shows that the thickness of the subsurface cobalt layer lies in the range 2–5 nm, which is of the

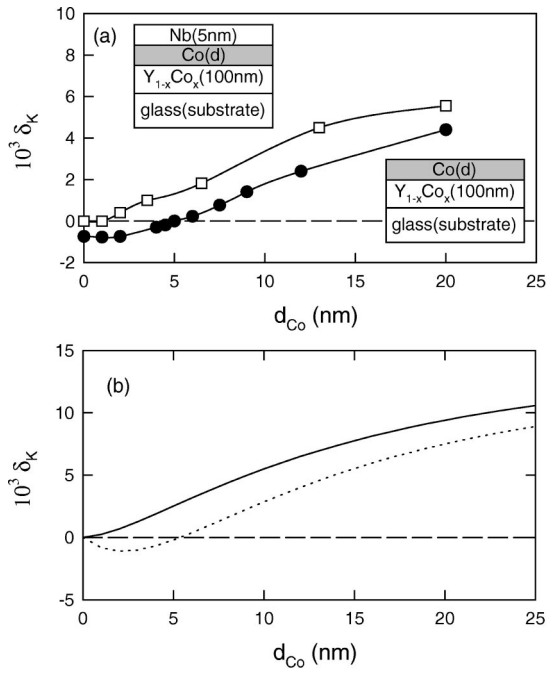

FIG. 7. (a) δ_K vs Co-layer thickness for Co(d)/$Y_{0.5}Co_{0.5}$ (100 nm)/glass(substrate) samples (filled symbols) and for Nb (5nm)/Co(d)/$Y_{0.5}Co_{0.5}$ (100 nm)/glass(substrate) samples (hollow symbols) at an incidence angle $\theta=72°$. Also shown are the sketches of the samples structure. (b) Simulated δ_K vs Co-layer thickness for Co(d)/Y(substrate) structures (dotted line) and Nb (5nm)/Co(d)/Y(substrate) structures (solid line).

same order as that found in the literature from threshold photoemission of spin-polarized electrons.[46]

These results are qualitatively predicted by our model [see Fig. 7(b), where a calculation of δ_K for nonmonochromatic light in a Co(film)/Y(substrate) structure is plotted (dotted line)]. δ_K is negative for small Co thickness and crosses zero at $d_{Co}=5$ nm, i.e., at the same value as in the Co/$Y_{0.5}Co_{0.5}$ experiment. The theoretical curve only differs from the experimental data below $d_{Co}=2$ nm, where a natural subsurface Co layer will be present in the real samples but that is not considered in the simulation. Here we used the approximation of taking the optical coefficient for $Y_{0.5}Co_{0.5}$ as that of yttrium. This is allowed because the influence of a nonmagnetic substrate on δ_K is not very critical on the qualitative behavior.

To avoid yttrium segregation and to assure the existence of a cobalt layer free from oxide, another experiment has been carried out. In this case the same Co/$Y_{1-x}Co_x$ structures have been grown, but now protected with a 5-nm-thick Nb top layer. The δ_K vs d_{Co} behavior for the Nb(5nm)/Co(d)/$Y_{1-x}Co_x$ samples is shown in Fig. 7(a) (hollow symbols). It should be stressed that, different than the previous case, δ_K is positive for all the cobalt thickness range in these protected samples. This behavior is again predicted by our model, as can be seen in the simulated curve of Fig. 7(b) (solid line). The main discrepancy between the experimental and the theoretical curve is the zero δ_K value found experimentally at $d_{Co}=1$ nm. This can again be explained in terms of interface magnetism. A $\delta_K=0$ value may be due to the presence of a dead-cobalt layer located at the Nb/Co interface for d_{Co} below 2 nm. This dead-layer thickness is of the same order as can be found in the literature[47] and, in fact, it has been verified by AGM magnetometry that the magnetization is zero for the sample with $d_{Co}=1$ nm. These results demonstrate the great utility of MOTKE when it is used in conjunction with magnetometry in the determination of interface magnetism.

VI. MULTILAYERS

One of the research fields where magneto-optical effects can provide more valuable information is in the study of magnetic multilayers. In particular, the issue of coupling between magnetic layers across nonmagnetic spacers has recently attained a high interest.[48] There are many multilayer systems, like Co/Cu (Ref. 24) or Fe/Cu,[49] that present an oscillatory magnetic coupling depending on the spacer layer thickness. In general, a straightforward interpretation of the dependence of the MOTKE signal in terms of the parallel or antiparallel alignment of the magnetizations of the individual layers (i.e., ferro or antiferromagnetic coupling) is not possible. Rather, the calculations of the detailed MOTKE response of a multilayer structure requires numerical simulations using the full model of Sec. III. In this section, we will discuss the conditions for the additivity of the MOTKE of the individual layers, which are found to be strongly dependent on the 3d metal present.

An approximate expression of the magneto-optical response of an antiferromagnetically coupled multilayer can only be derived in the simplest case of a bilayer, that is, of a structure that consists in two films with the same width d magnetized in opposite directions, on a thick nonmagnetic substrate. In order to obtain a simple analytical expression for δ_K we have taken $N_2=N_3=N_4=N$, $Q_2=-Q_3$. Once more, we have obtained the same expression for δ_K than that of a thick layer [given by Eq. (29)] in which the magneto-optic constant is replaced by an effective constant

$$Q_{\mathrm{eff}}=Q\left[1-\exp\left(i\frac{2\omega d}{c}\sqrt{N^2-\sin^2\theta_1}\right)\right]^2. \qquad (37)$$

For thin enough layers, this Q_{eff} is proportional to $(d/\lambda_0)^2$. This implies that there is a cancellation of the MOTKE of the oppositely magnetized layers, at least, to first order in d/λ_0.

On the other hand, the presence of a nonmagnetic spacer between the magnetic layers introduces additional phase factors in the calculation that can result in strong deviations from this simple result, as shown in Fig. 8 for several Co/Cu/Co trilayers. This figure is a contour plot of the calculated δ_K values as a function of the individual layer thicknesses. The simulated structures are Co(n)/Cu(N)/Co(m)/Cu(substrate) trilayers, where the layer thicknesses are given in terms of the number of atomic layers (i.e., in multiples of the lattice constants $a_{Co}=2.51$ Å and $a_{Cu}=3.61$ Å). m is the number of Co atomic layers grown on top of the Cu substrate and n is the number of atomic layers in the upper film of the structure. The Cu spacer thicknesses considered are $N=3$, 6, 9, and 12 atomic layers, which correspond to the experimentally reported range of values for either ferromagnetic (F),

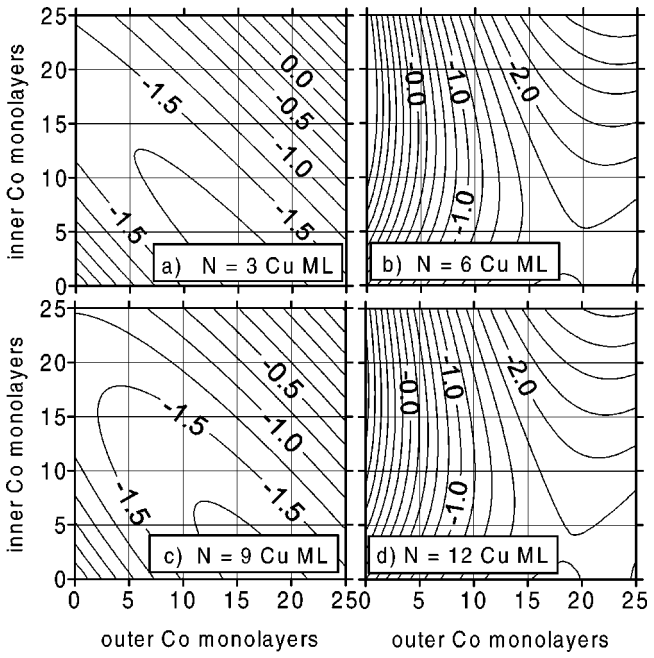

FIG. 8. Contour plot of δ_K values simulated for several Co(n)/Cu(N)/Co(m)/Cu(substrate) structures at $\theta=70°$: (a) $N=3$, ferromagnetic alignment; (b) $N=6$, antiferromagnetic alignment; (c) $N=9$, ferromagnetic alignment; (d) $N=12$, antiferromagnetic alignment. The horizontal and vertical axes correspond to n and m, the number of atomic Co planes in the surface and interior layers, respectively. To define the sign of δ_K, the positive direction of the magnetization has been chosen to be that of the upper Co layer.

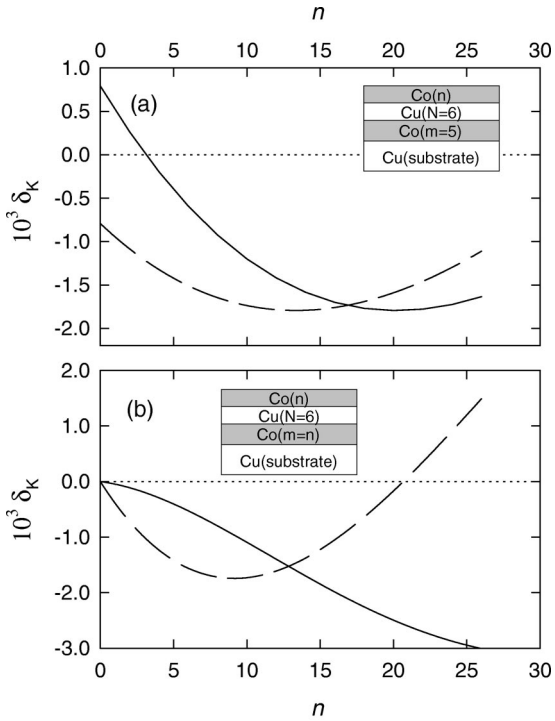

FIG. 9. (a) δ_K vs n for Co(n)/Cu($N=6$)/Co($m=5$)/Cu(substrate) structure at $\theta=70°$ with different configurations of the magnetization in the Co layers: solid line, antiparallel alignment; dashed line, parallel alignment. (b) δ_K vs n for a symmetric Co(n)/Cu($N=6$)/Co(n)/Cu(substrate) structure at $\theta=70°$: solid line, antiparallel configuration; dashed line, parallel configuration. Note the nonzero δ_K value, in spite of the zero total magnetization. Also shown are the sketches of the simulated structures.

$N=3$ and 9, or antiferromagnetic (AF), $N=6$ and 12, coupling in Co/Cu superlattices.[24] The angle of incidence is $\theta=70°$ and $\lambda=670$ nm. The positive sense of the magnetization is chosen to be that of the upper layer, in order to define the sign of δ_K. Bulk values of the optic and magneto-optical constants of Cu and Co are used in the calculation. It is worth to note that polar Kerr effect measurements in Co/Cu multilayers[41] in this thickness range have only found some changes in the refractive index of Cu due to interface effects, while the bulk constants of Co could be used as a good approximation down to subnanometer thicknesses. In any case, the qualitative response presented here is not very sensitive to the optical constants of the Cu intermediate layer.

In the F structures of Figs. 8(a) and 8(c) the total magnetization M_F is proportional to $n+m$ so that the lines of constant M_F are parallel to the $n=-m$ diagonal. This behavior is only observed in a limited region of the δ_K contour plot. Also, in the AF trilayers of Figs. 8(b) and 8(c), the total magnetization M_{AF} is proportional to $n-m$, so that the magnetic behavior is symmetric in the line $n=m$. However the calculated δ_K is nonsymmetric along the diagonal of Figs. 8(b) and 8(c), reflecting the nonlinear dependence of δ_K on $n-m$.

In order to get a better idea of the influence of the nonlinearities of δ_K on the MOTKE hysteresis loops, it is interesting to take a closer look at the behavior of one of these structures both at saturation (F alignment) and at remanence (AF alignment). For example, Fig. 9(a) shows δ_K vs n for a Co(n)/Cu($N=6$)/Co(m)/Cu(substrate) trilayer along a line of constant $m=5$ both for the parallel and antiparallel alignment of the magnetization of the individual layers. These two curves would correspond to the δ_K values at saturation [δ_K(F)] and at remanence [δ_K(AF)], respectively. In both cases, δ_K has a nonlinear behavior and can take positive and negative values, in a similar way to the thin Co film grown on a metallic Y substrate presented in Sec. IV B. Even more, in the symmetric trilayer case (i.e. $n=m$ and $N=6$) shown in Fig. 9(b), δ_K(AF) is only zero for very small Co thicknesses ($n\approx 1$) and then decreases to negative values that can become as large as δ_K(F) for $n>15$. That is, a nonvanishing δ_K value is found in structures with zero magnetization, confirming the nonadditive character of the MOTKE in the Co/Cu system. On the other hand, due to this lack of compensation in the AF configuration, the actual sign of δ_K(AF) in this symmetric structure depends on the relative sign of the individual layers magnetization respect to the saturating field. Thus, MOTKE could be used to analyze the rotations in the individual layers, even in this configuration of zero magnetic moment.

Another multilayer system where the literature[49] reports a sign change of the magnetic coupling are Fe/Cu/Fe trilayers grown on Cu substrates, the coupling being ferromagnetic for Cu layer thickness less than 8 monolayers and antiferro-

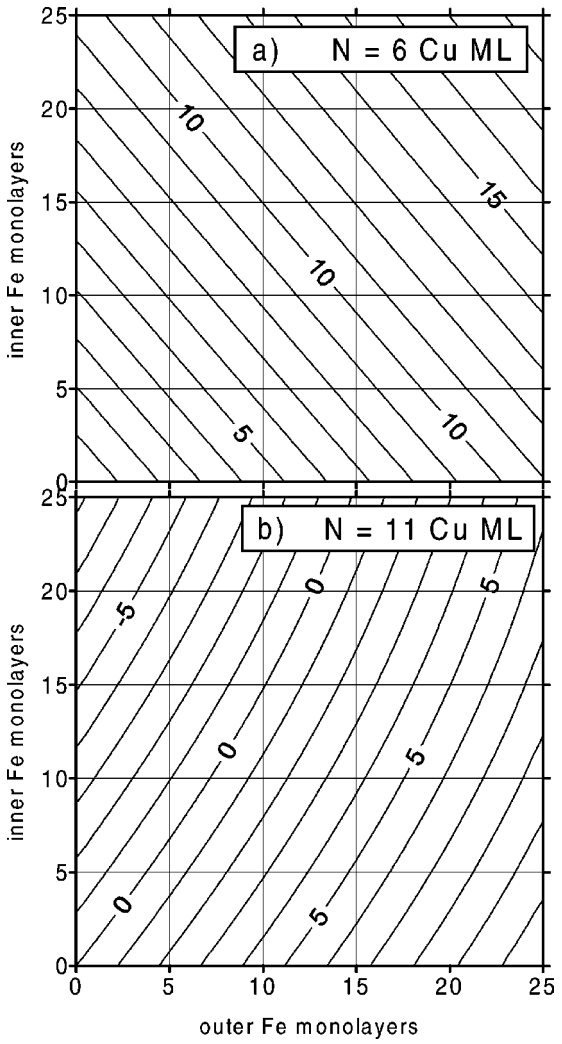

FIG. 10. Contour plot of δ_K values simulated for an Fe(n)/Cu(N)/Fe(m)/Cu(substrate) structure at $\theta=70°$: (a) parallel configuration and $N=6$; (b) antiparallel configuration and $N=11$. The horizontal and vertical axes correspond to n and m, the number of atomic Fe planes in the surface and interior layers, respectively. To define the sign of δ_K, the positive direction of the magnetization has been chosen to be that of the upper Fe layer.

magnetic in the range 9–13 monolayers. Figures 10(a) and 10(b) show the theoretical results that correspond to $N=6$ with ferromagnetic coupling and $N=11$ with antiferromagnetic coupling. It can be checked in both cases that, though the behavior of δ_K is never strictly additive, the deviation from linearity is clearly lesser compared to that of Co/Cu trilayers.

The differences found in these two magnetic multilayer systems can be related to the different behavior of δ_K for a simple magnetic film grown on a metal substrate that depends strongly on the 3*d* metal used (shown in Fig. 5). The complex behavior of the Co/Cu system described in Figs. 8 and 9 is associated with the presence of phase factors in the calculation that also give rise to the nonlinear dependence of δ_K of a Co(film)/Y(substrate) structure. On the other hand, additivity between the contributions of the individual layers is favored in the Fe/Cu system by the initial linear slope of δ_K vs d in Fe(film)/Y(substrate) structures. In general, the most important conclusion from these simulations is that the MOTKE in multilayers is never strictly additive, i.e., it is not proportional to the sample magnetic moment. Therefore, each particular case must be analyzed in order to obtain significant information from the MOTKE signal in magnetic multilayers.

VII. CONCLUSIONS

A theoretical model based on a phenomenological permittivity tensor has been developed to predict the magneto-optical transverse Kerr effect in multilayers. The obtained results clearly exhibit the complex behavior characteristic of this effect. In some simple cases, such as a thin metal film on a metallic substrate approximate analytic expressions can be derived in terms of an effective magneto-optical constant Q_{eff}. This approach allows to get a better insight into the origin of the anomalous thickness dependence of the MOTKE signal. The comparison between simulated and experimental behavior in the Y/Co system shows how this nonlinear character makes MOTKE a very useful tool to obtain an accurate determination of the magneto-optical constants of the material.

The complexity of the MOTKE response can also be used as an advantage with respect to other magneto-optic effects in the study of surface and interface magnetism. As an example, surface Y/Co segregation in $Y_{1-x}Co_x$ alloys has been studied. It is found that a 2–5 nm thick Co-enriched subsurface layer is easily detected and characterized by this technique in combination with bulk magnetometry. Finally, numerical simulations of the MOTKE in magnetic multilayer systems (Co/Cu and Fe/Cu) show that, even though the contributions from the individual layers are never strictly additive, the nonlinearity in the behavior is strongly dependent on the 3*d* metal used. In particular, a more complex behavior is expected in Co-based multilayers than in Fe-based systems. On the other hand, one of the consequences of the nonlinearity of the MOTKE is the nonvanishing δ_K value for samples with zero net magnetization. Therefore, this technique could be used to probe the alignment of the individual layers even in a configuration of vanishing magnetic moment.

ACKNOWLEDGMENTS

This work has been supported by the Spanish CICYT (Grant No. MAT99-0724).

APPENDIX: APPROXIMATE ANALYSIS OF A MAGNETIC FILM ON A METAL SUBSTRATE

The magneto-optic behavior of δ_K for a bilayer made of a magnetic thin layer of constants N and Q and thickness d grown on a nonmagnetic metal substrate with index N can be represented by an effective constant

$$Q_{\mathrm{eff}} \simeq Q[1-\exp(i2\omega dN/c)], \tag{A1}$$

since, for metals, $|N^2| \gg 1$. Expression (A1) implies that, even though the magnetooptical response is linear in Q, it has a nontrivial dependence on the magnetic layer thickness. There is a simple physical reason for this lack of linearity. In the MOTKE configuration both the phase and amplitude of the linearly polarized light propagating in the medium are modified due to the presence of the magnetization. For a semi-infinite medium, only the change in amplitude is observed by the change of reflectivity that can be assumed to be, in first order, proportional to the net magnetization.[12] However, as soon as interfaces are introduced in the sample structure, the total reflected wave is the result of the multiple interference from the partial waves reflected at each layer, with additional phase factors introduced by the light propagation in the consecutive layers. Therefore, there is not, in general, a simple linear relation linking the intensity of the light reflected from the total structure with the intensity of the light coming from each layer, i.e., linking δ_K with the magnetic moment of the multilayer. Strict linearity will only be found in the particular simple case of a thin-magnetic film on a metallic substrate for very small magnetic layer thickness. In this case a simplified expression for δ_K can be derived from Eq. (30) by substituting Q_{eff} for Q_2 and taking the limit $d \simeq 0$. Thus,

$$\delta_K \simeq \frac{8\omega d}{c} \sin 2\theta_1 \, \mathrm{Re}\left(\frac{QN(1+i\omega dN/c)}{N^2 \cos^2\theta_1 - 1} \right) \tag{A2}$$

from which the slope of the $\delta_K(d)$ vs d at $d=0$ can be derived. Aiming to analyze the qualitative features of δ_K suffice it to observe that this quantity is proportional to the cosine of the argument of a complex expression $h(d)$. Thus, the slope of $\delta_K(d)$ at $\delta_K = 0$ has the same sign than $\cos\phi_0$, where ϕ_0 is the argument of

$$h_0 \equiv \frac{QN}{N^2 \cos^2\theta_1 - 1}. \tag{A3}$$

On the other hand, for a thick-magnetic layer $Q_{\text{eff}} \simeq Q$, δ_K is proportional to $\cos\phi_\infty$, ϕ_∞ being the argument of the complex quantity

TABLE II. Calculated values of $\cos\phi_0$ and $\cos\phi_\infty$ for transition metals at $\lambda = 670$ nm and angle of incidence $\theta_1 = 70°$.

	Co	Fe	Ni
$\cos\phi_0$	−0.08	1	−0.42
$\cos\phi_\infty$	0.42	0.75	0.04

$$h_\infty \equiv \frac{iQ}{N^2 \cos^2\theta_1 - 1} = \frac{ih_0}{N}. \tag{A4}$$

Table II shows the values of the cosine of the arguments of h_0 and h_∞ for the three $3d$ metals. A look at this table shows that δ_K is a decreasing function of the thickness of the magnetic layer (at $d=0$) for Co and Ni, and an increasing one for Fe (see Fig. 5). The lack of a linear part in the graph of δ_K vs d for Co is due to the fact that ϕ_0 differs from $-\pi/2$ in 0.08 rad; hence, only a small increase in thickness is needed to drive the argument of $h(d)$ above $-\pi/2$ and, therefore, to change the sign of δ_K. On the contrary, the high values attained by $\cos\phi_0$ for Fe and Ni suggest for a linear dependence of δ_K vs d whilst $\exp(-4\pi\kappa d/\lambda)$ can be substituted by a series expansion until first-order terms. Another consequence of this analysis is that since $\cos\phi_\infty > 0$ for Co and Ni, δ_K must cross zero at some thickness. The particular value of the zero crossing will be much larger for Ni than for Co, since a supplementary phase must be added.

The small value of $\cos\phi_0$ for Co suggests that the actual value of δ_K may be very sensitive to the small phases neglected in the calculation. In particular, certain sensitivity to the actual metallic substrate is to be expected. On the other hand, the small value of $\cos\phi_\infty$ for Ni reveals that the bulk value of δ_K must be much lesser than that of the other two cited transition metals at this wavelength.

In summary, the different MOTKE responses of thin films of $3d$ metal grown on metallic substrates cannot be simply related with their magnetic moments (i.e., with the product of magnetization times thickness). Rather, they are determined by the physics of light propagation in each magnetic material, i.e., by the particular values of the optic and magneto-optic constants and by the refraction and reflection effects associated with the presence of interfaces in the sample structure.

[1] J. L. Erksine and E. A. Stern, Phys. Rev. B **8**, 1239 (1973).

[2] C. N. Afonso, F. Briones, and S. Giron, Solid State Commun. **43**, 105 (1982).

[3] Yu A. Uspenskii, E. T. Kulatov, and S. V. Halilov, Phys. Rev. B **54**, 474 (1996).

[4] Y. U. Idzerda, L. H. Tjeng, H. J. Lin, C. J. Gutierrez, G. Meigs, and C. T. Chen, Phys. Rev. B **48**, 4144 (1993).

[5] E. R. Moog and S. D. Bader, Superlattices Microstruct. **1**, 543 (1985).

[6] J. Araya-Pochet, C. A. Ballentine, and J. L. Erksine, Phys. Rev. B **38**, 7846 (1988).

[7] C. Shearwood, S. J. Blundell, M. J. Baird, J. A. C. Bland, M. Gester, H. Ahmed, and H. P. Hughes, J. Appl. Phys. **75**, 5249 (1994).

[8] O. Geoffroy, D. Givord, Y. Otani, B. Pannetier, A. D. Santos, M. Schlenker, and Y. Souche, J. Magn. Magn. Mater. **121**, 516 (1993).

[9] P. Vavassori, O. Donzelli, V. Metlushko, M. Grimsditch, B. Ilic, P. Neuzil, and R. Kumar, Phys. Rev. B **88**, 999 (2000).

[10] M. Velez, R. Morales, J. M. Alameda, F. Briones, J. I. Martin, and J. L. Vicent, J. Appl. Phys. **87**, 5654 (2000).

[11] A. K. Zvezdin and V. A. Kotov, *Modern Magnetooptics and Magnetooptical Materials* (Institute of Physics, Bristol, 1997), pp. 5 and 47.

[12] See, e.g., A. V. Sokolov, *Optical Properties of Metals* (Blackie and Son, Ltd., London, 1967).
[13] J. M. Florczak and E. D. Dahlberg, J. Appl. Phys. **67**, 7520 (1990).
[14] W. B. Zeper, F. J. A. M. Greidanus, P. F. Carcia, and C. R. Fincher, J. Appl. Phys. **65**, 4971 (1989).
[15] R. Atkinson, S. Pahirathan, I. W. Salter, P. J. Grundy, C. J. Tatnall, J. C. Lodder, and Q. Meng, J. Magn. Magn. Mater. **162**, 131 (1996).
[16] L. M. Alvarez-Prado, G. T. Perez, R. Morales, F. H. Salas, and J. M. Alameda, Phys. Rev. B **56**, 3306 (1997).
[17] M. Pohtl, W. Herbst, H. Pascher, W. Faschinger, and G. Bauer, Phys. Rev. B **57**, 9988 (1998).
[18] W. J. Antel, F. Perjeru, and G. R. Harp, Phys. Rev. Lett. **83**, 1439 (1999).
[19] E. E. Shalyguina and K. H. Shin, J. Magn. Magn. Mater. **220**, 167 (2000).
[20] For a review see S. Bader, J. Magn. Magn. Mater. **100**, 440 (1991).
[21] Y. B. Xu, E. T. M. Kernohan, D. J. Freeland, A. Ercole, M. Tselepi, and J. A. C. Bland, Phys. Rev. B **58**, 890 (1998).
[22] S. S. Kang, W. Kuch, and J. Kirschner, Phys. Rev. B **63**, 024401 (2000).
[23] Z. Q. Qiu, J. Pearson, A. Berger, and S. D. Bader, Phys. Rev. Lett. **68**, 1398 (1992).
[24] A. Cebollada, R. Miranda, C. M. Schneider, F. Schuster, and J. Kirschner, J. Magn. Magn. Mater. **102**, 25 (1991).
[25] D. E. Burgler, D. M. Schaller, C. M. Schmidt, F. Meisinger, J. Kroha, J. McCord, A. Hubert, and H. J. Guntherodt, Phys. Rev. Lett. **80**, 4983 (1998).
[26] R. K. Kawakami, E. Rotenberg, E. J. Escorcia-Aparicio, H. J. Choi, J. H. Wolfe, N. V. Smith, and Z. Q. Qiu, Phys. Rev. Lett. **82**, 4098 (1999).
[27] G. J. Strijkers, J. T. Kohlhepp, and W. J. M. Jonge, Phys. Rev. Lett. **84**, 1812 (2000).
[28] K. R. Heim and M. R. Scheinfein, J. Magn. Magn. Mater. **154**, 141 (1996).
[29] A. Hubert and G. Traeger, J. Magn. Magn. Mater. **124**, 185 (1993).
[30] J. Zak, E. R. Moog, C. Liu, and S. D. Bader, J. Magn. Magn. Mater. **89**, 107 (1990).
[31] R. Atkinson and P. H. Lissberger, J. Magn. Magn. Mater. **118**, 271 (1993).
[32] J. M. Alameda and F. Lopez, Phys. Status Solidi A **69**, 757 (1982).
[33] K. O'Grady, V. G. Lewis, and D. P. E. Dickson, J. Appl. Phys. **73**, 5608 (1993).
[34] G. S. Krinchik and G. M. Nurmukhamedov, Zh. Éksp. Teor. Fiz. **48**, 34 (1965) [Sov. Phys. JETP **21**, 22 (1965)].
[35] D. H. Martin, K. F. Neal, and T. J. Dean, Proc. Phys. Soc. London **86**, 605 (1965).
[36] L. D. Landau and E. M. Lifshitz, *Electrodynamics of Continuous Media* (Pergamon, London, 1960).
[37] F. Briones, Tesis Doctoral, Universidad Complutense, Madrid, 1972.
[38] Y. Suzuki, T. Katayama, S. Yoshida, K. Tanaka, and K. Sato, Phys. Rev. Lett. **68**, 3355 (1992); R. Megy, A. Bounouh, Y. Suzuki, P. Beauvillain, P. Bruno, C. Chappert, B. Lecuyer, and P. Veillet, Phys. Rev. B **51**, 5586 (1995).
[39] G. S. Bains, R. Carey, D. M. Newman, and B. W. J. Thomas, J. Magn. Magn. Mater. **104-107**, 1011 (1992).
[40] *Handbook of Chemistry and Physics*, 78th ed. edited by D. R. Lide (CRC Press, Boca Raton, 1997); K. H. J. Buschow, in *Ferromagnetic Materials*, edited by E. P. Wohlfarth and K. H. J. Buschow (Elsevier, Amsterdam, 1988), Vol. 4; P. B. Johnson and R. W. Christy, Phys. Rev. B **9**, 5056 (1974).
[41] R. Atkinson and P. M. Dodd, J. Magn. Magn. Mater. **173**, 202 (1997).
[42] P. E. Ferguson and R. J. Romagnoli, J. Appl. Phys. **40**, 1236 (1969).
[43] J. Zak, E. R. Moog, C. Liu, and S. D. Bader, Appl. Phys. Lett. **58**, 1214 (1991).
[44] F. H. Salas, C. Dehesa, G. T. Pérez, and J. M. Alameda, J. Magn. Magn. Mater. **121**, 548 (1993).
[45] J. M. Alameda, M. C. Contreras, and A. R. Lagunas, J. Magn. Magn. Mater. **72**, 279 (1988).
[46] G. L. Bona, F. Meier, M. Taborelli, H. C. Siegman, A. Bell, R. Gambino, and E. Kay, J. Magn. Magn. Mater. **54-57**, 1043 (1986).
[47] Th. Muhge, K. Theis-Brohl, K. Westerholt, H. Zabel, N. N. Garif'yanov, Yu. V. Goryunov, I. A. Garifullin, and G. G. Khaliullin, Phys. Rev. B **57**, 5071 (1998).
[48] P. Grunberg, R. Schreiber, Y. Pang, M. B. Brodsky, and H. Sowers, Phys. Rev. Lett. **57**, 2442 (1986); S. S. P. Parkin, N. Moore, and K. P. Roche, *ibid.* **64**, 2304 (1990).
[49] B. Heinrich, Z. Celinski, K. Myrtle, J. F. Cochran, A. S. Arrott, and J. Kirschner, J. Magn. Magn. Mater. **93**, 75 (1991).